

Structure of rolled CuTi4 alloy

J. Konieczny ^{a,*}, Z. Rdzawski ^{a,b}

^a Institute of Engineering Materials and Biomaterials, Silesian University of Technology, ul. Konarskiego 18a, 44-100 Gliwice, Poland

^b Institute of Non-Ferrous Metals, ul. Sowińskiego 5, 44-100 Gliwice, Poland

* Corresponding e-mail address: jaroslaw.konieczny@polsl.pl

Received 17.11.2011; published in revised form 01.01.2012

Materials

ABSTRACT

Purpose: The aim of the work is to investigate the microstructure of the heat treated and cold rolled commercial CuTi4 copper alloy.

Design/methodology/approach: Observations and investigations of the structure were made on the JOEL transmission electron microscope (TEM), scanning electron microscope (SEM) Zeiss SUPRA 25 and diffractometer X'Pert Panalytical.

Findings: Decomposition of supersaturated solid solution in that alloy is similar to the alloys produced in laboratory scale. The observed differences in microstructure after supersaturation were related to the presence of undissolved Ti particles and increased segregation of titanium distribution in copper matrix including microareas of individual grains. The mentioned factors influence the mechanism and kinetics of precipitation and subsequently the produced wide ranges of functional properties of the alloy.

Research limitations/implications: Cold deformation (50% reduction) of the alloy after supersaturation changes the mechanism and kinetics of precipitation and provides possibilities for production of broader sets of functional properties. It is expected that widening of the cold deformation range should result in more complete characteristics of material properties, suitable for the foreseen applications. Similar effects can be expected after application of cold deformation after ageing.

Practical implications: The elaborated research results present some utilitarian qualities since they can be used in development of process conditions for industrial scale production of strips from CuTi4 alloy of defined properties and operating qualities.

Originality/value: The mentioned factors influence the mechanism and kinetics of precipitation and subsequently the produced wide ranges of functional properties of the Cu-Ti alloys.

Keywords: Metallic alloys; Electron microscopy; Heat treatment; CuTi4 alloy

Reference to this paper should be given in the following way:

J. Konieczny, Z. Rdzawski, Structure of rolled CuTi4 alloy, Journal of Achievements in Materials and Manufacturing Engineering 50/1 (2012) 26-39.

1. Introduction

Copper alloys composed with different elements and improvement of production technology which create new possibilities in the technical demand. Nowadays, they are widely applied and most commonly used alloys in the group of non-ferrous metals [1-10].

Mechanical properties of pure metals are lower than mechanical properties of solid solutions. Introduction of the foreign element into the parent metal results with reinforcing of this metal, which is caused by interaction of dislocations with the foreign atoms. Mechanical properties of copper alloys are improved by a small addition - of up to 3% - of alloying elements which, however, reduce the electrical conductivity to a different extent. These alloys are traditionally named high-alloyed coppers.

Copper alloys with addition of beryllium called traditionally the beryllium copper [11] which, apart from their high toxicity and technological problems with its fabricating and processing [12], are widely used because of their advantageous mechanical properties, as well as their corrosion- and abrasion wear resistance. Works on Cu-Ti alloys are, among others, the effect of search for the Cu-Be alloys' substitutes. The CuTi alloys compared to the beryllium copper are characteristic of the similar electrical properties and comparable mechanical ones.

Moreover, the widely used method for improvement of the mechanical properties of metal alloys is their reinforcing with particles of new phases precipitated during ageing. The more uniform is the distribution of the nano-scale reinforcing phase particles the more intensive is its reinforcing effect. Precipitation at grain boundaries and crystal lattice defects may feature the obstacle which partially hinders the reinforcement mechanism. The reason is lowering the nucleation energy barrier by the defects. To eliminate the effect of the crystalline structure imperfections on the precipitation process the thermodynamic condition must be satisfied: no nucleation energy barrier. It is met inside of spinodals [13].

No precipitations occur at grain boundaries in the structure of alloys which is formed as a result of the spinodal transformation, and therefore, there are no lean zones in their vicinity. Such alloys are characteristic of the very good mechanical properties. The Cu-Ti alloys may be a good example, acquiring mechanical properties comparable to beryllium copper after the alternate heat treatment and plastic working [13].

The most effective way to improve the strength properties of the CuTi alloys is their precipitation hardening connected with strain hardening. Therefore, the intensive investigation is ongoing of the effect of the joint (alternate) heat treatment and plastic working, or heat treatment with cold working between the supersaturation- and ageing operations and after ageing [14-16]. It is worthwhile to mention that the spinodal transformation is of crucial importance here.

In the Cu-Ti alloys the spinodal decomposition takes place first and next areas enriched with titanium get ordered [17]. The modular lattice developing during ageing demonstrates good mechanical properties. The appropriate thermo-mechanical treatment consisting in deformation of the supersaturated alloys before their ageing ensures obtaining the tensile strength of above 1300 MPa [18]. The advantages of these alloys are good workability after ageing and the possibility to use the higher ageing temperature compared to other copper alloys [19].

Sato was the first one to carry out investigations of Cu-Ti alloys using the transmission electron microscope [20]. It was found out based on investigations carried out that the very big number of fine coherent precipitations distributed evenly in the matrix were observed in the CuTi3 alloy after ageing at temperature of 500°C as soon as after 10 min. The discontinuous transformation occurred during further ageing, whose front was moving through the matrix containing the uniformly distributed coherent particles, leaving the cellular structure behind. The investigations resulted also with detecting the metastable phase, whose precipitation was revealed already with the X-ray methods.

Datta and Soff found out [21], examining phase transformations occurring during ageing in CuTi4 alloy, that

ordering in areas enriched with Ti accompanies the spinodal transformation, which leads to formation of the $D1_a$ superlattice. The Cu_4Ti phase forms in these areas, which Knights and Wilkes [22] defined as the superlattice crystallizing in the $L1_2$ - Cu_3Au system with the lattice parameter $a=0,41$ nm. However, further investigations of Laughlin and Cahn [23,24] revealed that this superlattice crystallizes in the $D1_a$ - Ni_4Mo system. They confirmed this way results of the earlier works of Hakkarainen [25]. This structure is the A1 structure derivative, in which copper crystallizes, and it can be obtained by population of every fifth $\{420\}$ plane with titanium atoms.

Depending on titanium content in Cu-Ti alloys supersaturation is carried out in the 700-950°C temperature range for up to 7 hours with the subsequent ageing at temperature of 400-600°C for 1 to 16 hours [26]. As an example, Nagarjuna and Srinivas supersaturated CuTi1.5 alloy at the temperature of 750°C for 2 h with the subsequent ageing at temperature of 400°C for 6 h, while CuTi4.5 alloy was supersaturated at temperature of 860°C for 2 h, and next aged at temperature of 400°C for 1 h [14].

Investigation of the effect of heat treatment carried out on CuTi4,2 alloy, which was supersaturated at temperature of 825°C for 2 h, and next aged at temperature of 375°C for 05-25 h acquiring structure with grain size of 60-70 μm [27].

Semboshi with associates [28] investigated CuTi1 alloy annealed after casting at temperature of 800°C for 24 h in vacuum. The alloy was subjected to plastic strain by cold drawing and wire was obtained 70 mm long with the diameter of 0.25 mm. The wires were supersaturated next at temperature of 800°C for 3 h, and aged later at temperature of 350°C for 1-1030 h in deuter (D_2) atmosphere under pressure of 0.08 MPa.

Similarly, in works of Blacha and associates [26,29] supersaturation of CuTi0.8 and CuTi2.2 alloys was carried out at temperatures of 750-900°C for 1-4 h and ageing at temperatures of 320-550°C for 4-24 h.

Wrapping up investigations carried out by various scientific centres, their main goal was to determine the effect of the heat treatment process parameters (mainly of the ageing time and temperature) and of the effect of chemical composition on mechanical- and physical properties of Cu-Ti alloys. Because of the commercial application of these alloys the significant drawback of the investigations carried out was focusing of the authors solely on the laboratory alloys whose chemical composition was very simple, as they contain only two elements: Cu and Ti. Generally, they are obtained by melting the charge materials with purity of 99.99% [26,29-32]. Some few exceptions in works on the commercial alloys only confirm this rule [33].

Moreover, the cited works refer to heat treatment technologies with ageing time of more than 12 hours and also often about 24 hours. Such treatment method increases the unit cost of the final product, and therefore,, it is no longer competitive in the market. That is why the authors focused on investigations of the commercial, industrial CuTi4 alloy.

The goal of this work was to determine the ageing time effect on microstructure and properties of CuTi4 alloy strain hardened with the 50% total reduction after supersaturation and next aged at temperature of 550°C for 1, 60, and 420 minutes.

2. Material and methods

Investigations were carried out on the commercially available CuTi4 alloy. Chemical composition of the industrial CuTi4 alloy is presented in Table 1.

The material preparation procedure for investigation of CuTi4 alloy included:

- hot working with 80% draft to 3.0 mm thickness,
- supersaturation (920°C/1h) in water,
- cold working with 50% draft,
- ageing at temperature of 550°C for 1 min, 60 min, and 420 minutes.

Examinations of microstructure and grains misorientation were made on ZEISS SUPRA 25 scanning electron microscope (SEM) using the EBSD (Electron Backscatter Diffraction Analysis) method and with JEOL 3010 transmission electron microscope (TEM).

Table 1.
Chemical composition of CuTi4 alloy

Cu	Ti	Zn	P	Pb	Sn	Mn	Ni	Sb	Bi	As	Cd
95.83	3.95	0.13	0.065	0.003	0.009	0.030	0.01	0.001	0.001	0.001	0.001

X-ray phase analysis of the specimens was made on Panalytical X'Pert diffractometer using filtered radiation of the lamp with cobalt anode. The measurement step was 0.05° and the impulse counting time was 10 sec.

3. Results and discussion

The maximum solubility of titanium in copper at temperature of 885°C is 8% at. (Fig. 1). The metastable intermediate phases with the ordered structure may originate before precipitation of the equilibrium β TiCu₄ phase. The peritectic reactions occurring between the melting point of the TiCu phase particles and the eutectic transformation temperature lead to origination of the Ti₃Cu₄, Ti₂Cu₃, TiCu₂, and TiCu₄ intermetallic phases. Moreover, two equilibrium TiCu₄ phases occur in CuTi alloys - stable β and metastable α . The α phase is transformed into β phase after long ageing (even at low temperature). Probably transformation is possible of β phase during cooling into the α one stable at low temperature [12].

Previous investigations [19] revealed that CuTi alloys can be precipitation hardened during ageing using the spinodal decomposition mechanism which causes structure clustering and ordering. Extensive research in precipitation mechanism in Cu-Ti alloys [34-36] indicated that the β' (Cu₄Ti) intermetallic phase adds to strengthening of matrix during ageing. Lengthy ageing of Cu-Ti alloys leads to cellular precipitation along the matrix grain boundary and forming (precipitation) of the β Cu₃Ti equilibrium phase [36-38].

The electron microscopy methods made the detailed phase components analysis possible of the CuTi4 alloy microstructure after its complex heat- and mechanical treatment composed of:

hot working → supersaturation → cold working → ageing

An important effect was revealed of the ageing time on morphology and size of the precipitated particles of the second phase (Figs. 2-7), using the transmission electron microscope methods in microstructure examinations of the CuTi4 commercial alloy aged at temperature of 550°C for 1 minute (variant 1) and for 420 minutes (variant 2).

Ageing of the supersaturated CuTi alloy containing about 4% Ti at. induces the spinodal decomposition accompanying precipitation of phases with the unordered structure, alternately enriched and impoverished with Ti.

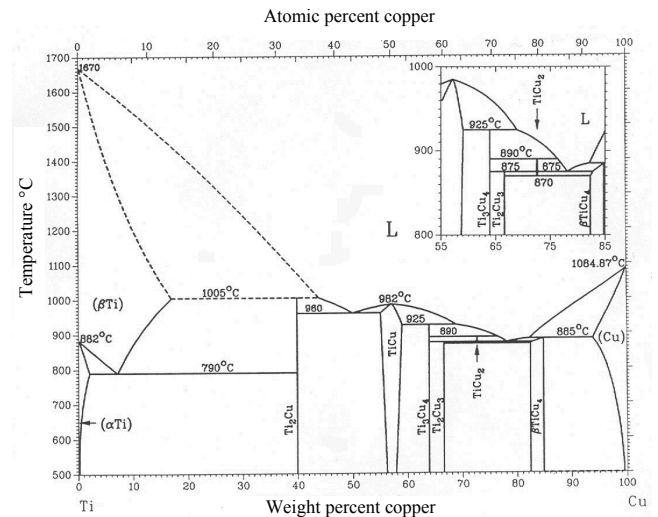


Fig. 1. Ti-Cu phase equilibrium system [39]

Diffraction patterns of these areas at the initial ageing stage indicate only to occurrences of the periodic stress in the lattice which is induced by the coherent particles/ Structure ordering in the titanium rich areas is possibly by reaching the relevant chemical composition.

Investigation results presented by Dutkiewicz [40-43] revealed that extension of the CuTi4 alloy ageing time leads to dissolving the precipitated particles of the second phase, which results with reduction of the alloy hardness.

As a result of the discontinuous transformation the Cu₃Ti equilibrium phase lamellae originate arranged alternately with the solid solution lamellae. The coherent precipitations originating as a result of the spinodal transformation are arranged periodically. Chemical composition and microstructure of the equilibrium phase are not unambiguously defined. Two types of the equilibrium phases are distinguished:

- the unordered, high-temperature β' phase,
- the ordered, low-temperature β phase.

The β' phase crystallizes in the hexagonal lattice, whereas the β phase in the rhomb lattice [14,15].

In metals with the A1 regular lattice, like copper, the dynamic recrystallization usually does not occur in the hot working process. The grainy structure of metal originates in this case as a result of re-polygonization and coalescence of subgrains with participation of dislocation climb. The grain size is described with the relationship [44] then:

$$d^{-1} = A + B \log Z \quad (1)$$

where:

A and B - constants,

$Z = \dot{\epsilon} \exp\left(\frac{Q}{RT}\right)$ - Zener-Hollomon parameter, where:

Q - process activation energy,

R - gas constant,

T - absolute temperature.

Supersaturation occurring next causes dissolving the phases in matrix (except the primary precipitations) and also the average grain size growth and deterioration of the mechanical properties connected with it.

Material strengthening by structure refinement, inducing, and cumulation of the point- and line defects of the crystal lattice occurs during the next process stage - cold working with 50% reduction.

It was found, based on analysis of the bright field observations, that the alloy matrix is copper crystallizing in the Fm-3m regular system.

Examinations of the alloy aged at temperature of 550°C for 1 min confirmed also presence of the deformation twins bands (Figs 2a and c) of Cu_3Ti phase crystallizing in the orthorhombic crystal system with the lattice parameters $a=0.2585$ nm, $b=0.4527$ nm, and $c=0.4351$ nm (Fig. 2b) in Cu matrix.

Matching of the crystal lattices and precipitations is coherent most often at the initial precipitation stage. An important effect on service properties of the precipitation hardened alloys have the type of precipitations with the particular structure and properties, as well as their morphology, which is defined by the shape of the precipitated phase particles, volume portions of the particular fractions, crystallographic relations in respect to matrix, surface development, and the reciprocal packing of precipitations [45].

To confirm the significant effect of the ageing time on morphology and dimensions of the precipitated particles of the second phase in the investigated CuTi alloy the image is presented of the observed area of the lamellar continuous precipitation (Figs. 3a and c), in which, based on electron diffraction (Figs. 3b and d), particles were identified of Cu_3Ti_2 phase crystallizing in the tetragonal lattice with lattice parameters $a=b=0.313$ nm and $c=1.395$ nm. Similar results were obtained in works [12,46].

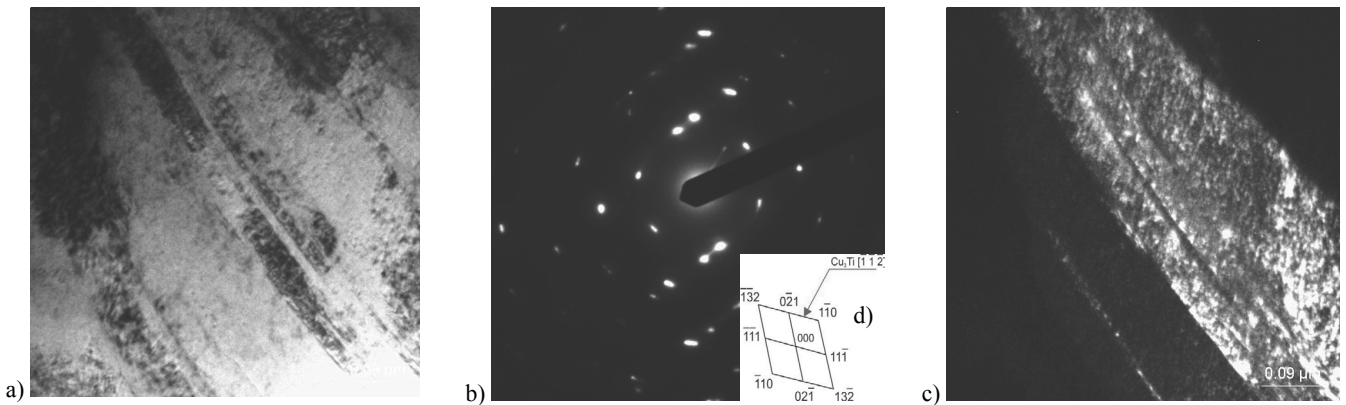


Fig. 2. Microstructure of CuTi4 alloy aged at temperature of 550°C for 1 minute a) bright field image; b) diffraction pattern from the area as in Figure a); d) solution of the diffraction pattern from Fig. b); c) dark field image from 021 reflection of Cu_3Ti (Cmcm space group)

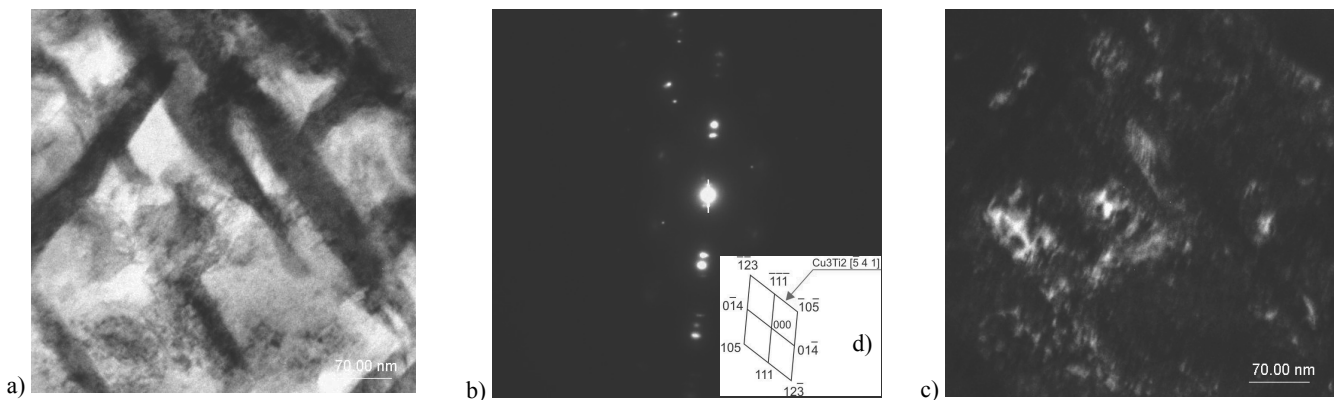


Fig. 3. Microstructure of CuTi4 alloy aged at temperature of 550°C for 1 minute a) bright field image; b) diffraction pattern from the area as in Figure a); d) solution of the diffraction pattern from Fig. b); c) dark field image from 111 reflection of Cu_3Ti_2 (P6₃/mmc space group)

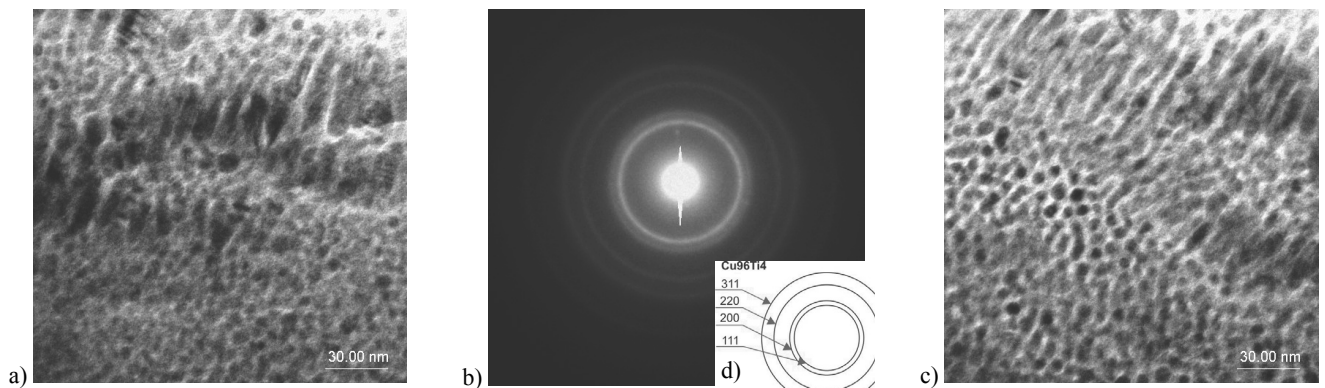


Fig. 4. Microstructure of CuTi4 alloy aged at temperature of 550°C for 1 minute, bright field image a), c) and f) boundary of the continuous- and discontinuous precipitations, b) diffraction pattern from area as in Figure a); d) solution of the diffraction pattern from Figures b

Next, in Figure 4 boundaries are presented between the continuous precipitation area with the visible discontinuous precipitation band, similar to the amorphous phase. Electron diffraction from the discontinuous precipitation area is of the unambiguously amorphous character, in which 4 circles were distinguished, and based on calculations and confrontation with data it was determined that they come from (111), (200), (220) and (311) planes of $\text{Cu}_{96}\text{Ti}_4$ phase, crystallizing in A1 cubic lattice (Fm-3m space group).

Spinodal decomposition, along with the accompanying structure changes, occurs in three particular cases [47]. The first one occurs in alloys aged in the 600-900°C temperature range for 100 hours, which were not deformed before. Next, the spinodal decomposition and continuous spinode precipitation take place in alloys which were previously deformed, aged at low temperature. The continuous precipitation extent (intensity) grows along with the ageing temperature rise. However, the spinodal decomposition, and continuous and discontinuous spinode precipitations take place in alloys which were previously deformed, aged at high temperature. The structure is non-homogeneous. Finally structure defects caused by deformation disappear [48-51].

Spinodal decomposition occurs spontaneously. There is no energetic barrier (thermodynamic one). It can be halted in the kinetic way only (slow diffusion, lattice coherence). There exists a distinguished wavelength of the composition fluctuation, which grows fastest (by the order of magnitude of 10 nm for metals).

The spinode wave length may be evaluated using Daniel-Lipson's relationship [52], based on the qualitative X-ray phase analysis comparing the obtained X-ray diffraction patterns for various ageing duration [53, 54]:

$$\lambda = \frac{ha_0}{h^2 + k^2 + l^2} \times \frac{\text{tg} \theta_B}{\Delta \theta} \quad (2)$$

where h, k, l are Miller indices of the Bragg peak, $\Delta \theta$ difference of the Bragg peak maximum location, θ_B is the Bragg angle value, a_0 is the lattice cell parameter for the homogenized alloy.

Area of the continuous precipitation in CuTi4 alloy microstructure is shown in Figure 5a. Next, b in Fig. 5b one of the continuous precipitation lamellae is presented, with the clearly visible twin, being most probably the heat treatment effect. Solution of the electron diffraction from the area shown in Fig. 5a made it possible to identify two phases occurring in this microstructure area - pure copper (Cu), crystallizing in the face-centred cubic lattice with lattice parameters $a=b=c=0.3615$ nm and the Ti- β allotropic form crystallizing in the B2 body-centred cubic lattice.

Figure 6 presents microstructure of CuTi4 alloy supersaturated from temperature 920°C (water cooling) next cold worked with 50% draft and aged at temperature of 550°C for 420 minutes. Deformation twins are clearly visible (Figs. 6a and c). Solution of the electron diffraction (Fig. 6b) made it possible to identify phase dominating in the deformation twin (Fig. 6c) as the metastable form of Ti- α titanium crystallizing in the hexagonal lattice with lattice parameters $a=b=46$ nm, $c=28.2$ nm [46] and second phase Cu_4Ti crystallizing in the orthorhombic system with lattice parameters $a=45.22$, $b=43.44$ nm and $c=128.97$ nm.

On the other hand, Figure 7 presents another microstructure area of CuTi4 alloy with the clearly visible deformation twin (Figs. 7a and c). Solution of the electron diffraction (Fig. 7b) made it possible to identify the phase as a pure copper (Cu), crystallizing in the face-centred cubic lattice with lattice parameters $a=b=c=0.3615$ nm [46].

Ageing time of the investigated material is of utmost importance to forming its final microstructure. The measurement results revealed that the high-angle boundaries' portion in the investigated microstructure grows along with extending the ageing time, at the expense of the small-angle boundaries' portion. As it results from the EBSD analysis (Table 2-4) of CuTi4 alloy hot worked alloy with 80% draft, next supersaturated (920°C/1h) in water, cold worked with 50% draft, and aged at temperature of 550°C for 1min, its small-angle (2-15°) boundaries' portion is above 61% in the investigated microstructure, while the remaining 38.9% are the high-angle (15-180°) boundaries. This attests to domination of large number of subgrains in the microstructure, which originated due to cold plastic strain, and too

short ageing time did not provide appropriate conditions for grain growth. On the other hand, the small-angle boundaries in the microstructure of the alloy aged finally at the temperature of

550°C for 420 min have only 15.8%, portion whereas the high-grained boundaries being the proof for increase in the number of annealing twins have more than 84% share in the structure.

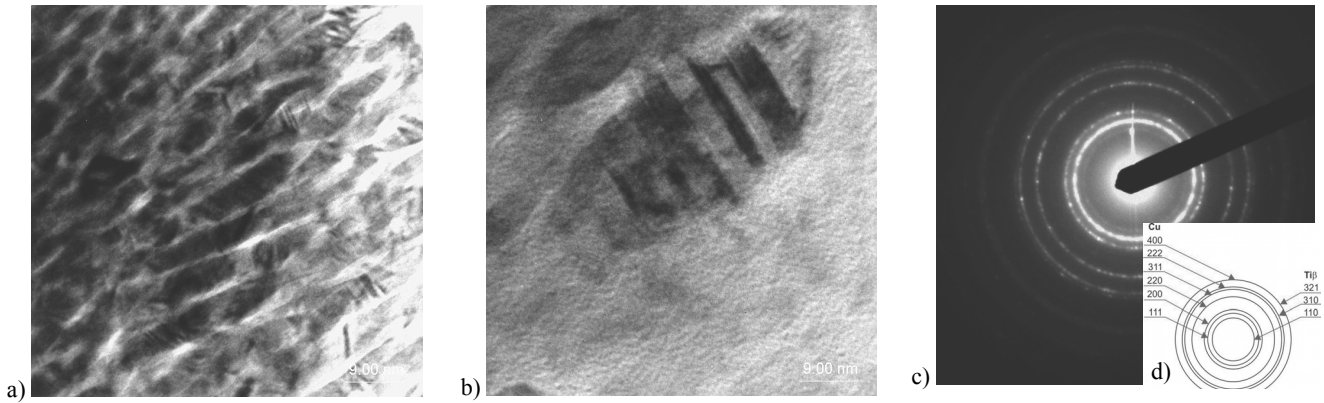


Fig. 5. Microstructure of CuTi4 alloy aged at temperature of 550°C for 1 minute; a) bright field image of the continuous precipitation; b) continuous precipitations with the visible annealing twin; c) diffraction pattern from the area as in Figure a; d) solution of the diffraction pattern

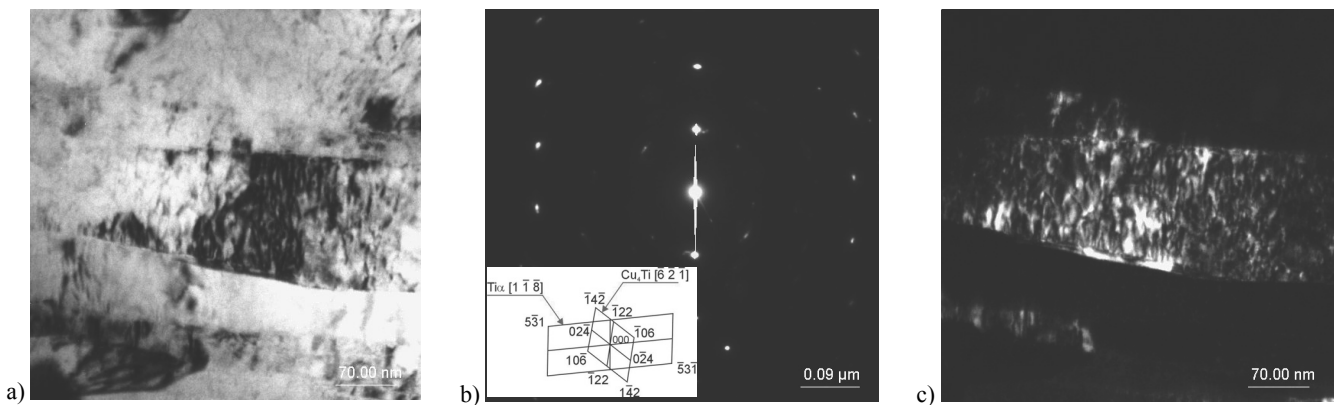


Fig. 6. Microstructure of CuTi4 alloy aged at temperature of 550°C for 420 minutes; a) bright field image; b) diffraction pattern from the area as in Figure a) and solution of the diffraction pattern; c) dark field image from 531 reflection of Ti α (P6/mmm space group)

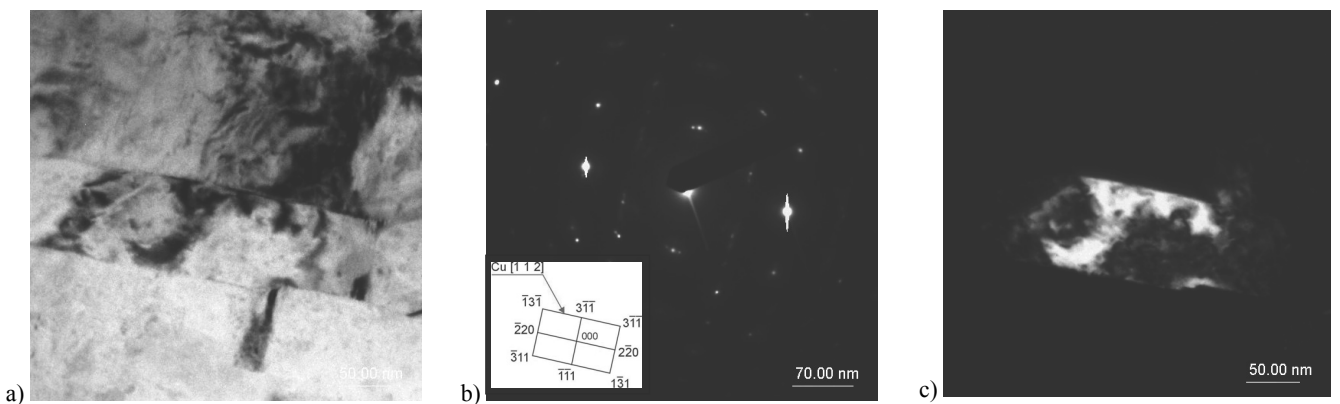


Fig. 7. Microstructure of CuTi4 alloy aged at temperature of 550°C for 420 minute a) bright field image; b) diffraction pattern from the area as in Figure a); d) solution of the diffraction pattern from Fig. b; c) dark field image from 220 reflection of Cu (Fm-3m space group)

Portions of the small- and high-angled boundaries after ageing for 60 minutes are presented to illustrate this process. More than 80% high-angle boundaries share in the microstructure is clearly visible. This attests the fact that in the investigated CuTi4 alloy, after the alternate plastic strain and heat treatment, the highest growth of the high-angled grains portion occurs during the first ageing hour, later this portion does not grow that fast.

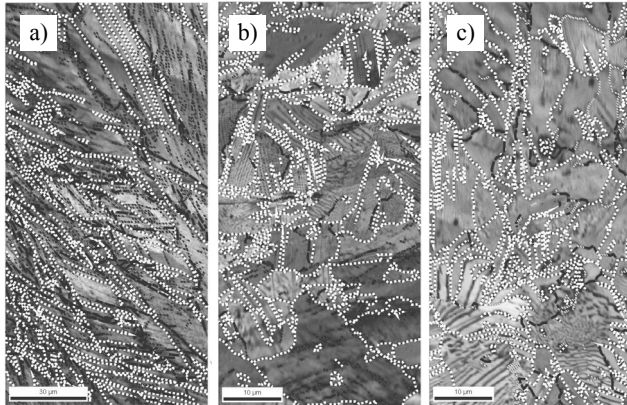


Fig. 8. Microstructure of CuTi4 alloy aged at temperature 550°C for a) 1 min, b) 60 min, c) 420 min; grains orientation maps using Euler angles - black dashed lines - small-angle boundaries, black dashed line - high-angle boundaries

Table 2.

CuTi4 alloy after supersaturation, 50% reduction, and ageing at temperature of 550°C for 1 minute (Fig. 8a)

	min	max	Portion [%]	Number of boundaries	Total length [mm]
-----	3°	5°	43.9%	35489	10.9
-----	5°	15°	17.2%	13912	4.02
-----	15°	180°	38.9%	31479	9.09

Table 3.

CuTi4 alloy after supersaturation, 50% reduction, and ageing at temperature of 550°C for 60 minutes

	min	max	Portion [%]	Number of boundaries	Total length [μm]
-----	2°	5°	12.4%	3309	382.09
-----	5°	15°	6.9%	1848	213.39
-----	15°	180°	80.7%	21553	2490.00

Table 4.

CuTi4 alloy after supersaturation, 50% reduction, and ageing at temperature of 550°C for 420 minutes

	min	max	Portion [%]	Number of boundaries	Total length [μm]
-----	2°	5°	7.4%	2626	227.42
-----	5°	15°	8.4%	2977	257.82
-----	15°	180°	84.2%	29912	2590.00

The wide-angle boundaries, that is boundaries with the large misorientation angle, to which twinned boundaries are included,

originate due to plastic strain (mechanical twins) and because of recrystallisation (annealing twins). The twinned boundaries developed because of the cold plastic strain - rolling, which was preceded by ageing of the investigated alloys, whereas the annealing twins originated during ageing.

Figs. 9-11 show EBSD analysis results as maps representing the reverse pole figures (texture representation). Comparing the drawings one can notice the evident fine-grained structure volume growth for the particular ageing conditions. One may suppose that the applied deformation accumulated in cold state in the material caused the further structure refinement for the investigated ageing conditions [55]. Microstructure refinement may probably be also caused by nucleation of grains in the primary recrystallisation process during ageing. Refinement of the microstructure with extension of the ageing time may prove it (Figs. 9-11).

As it turns out from Fig. 12a, in the microstructure of CuTi4 alloy aged at temp. 550°C for 1 minute, grains with the size of up to 22 μm have the biggest share, and the biggest grains with diameters from 44 to about 50 μm are as much as 15% (Tab. 5).

Next, in the microstructure of CuTi4 alloy aged for 60 or 420 minutes, grains with sizes of up to 14 μm have the biggest portion, 72.9 and more than 87%, respectively (Table 6 and 7). Moreover, in both cases the maximum grain size is slightly above 19 μm.

Wrapping up, grains with sizes of up to 22 μm after 1 minute long ageing feature 66% of the examined microstructure, whereas, in other cases they have 100% share. No bigger grains were revealed in the observed microstructure after 60 minutes (Fig. 12b) and after 420 min (Fig. 12c) of ageing. This proves unambiguously that at temperature of 550°C the primary recrystallisation phenomenon occurs, along with the time extension in the investigated period, realised by the nucleation mechanism of the new grains.

Nucleation of grains with sizes much smaller than those after 1 minute of ageing is connected undoubtedly with the ongoing primary recrystallisation process occurring in the solid solution without any changes of the initial phase and transformation product. Growth of the recrystallisation nuclei takes place by movement of the high-angle grain boundaries. Migration of the high-angle grain boundaries (Tables 2-4) is caused by the difference of atoms transitions through the energy barrier of the recrystallisation front G_m from the plastically deformed matrix to the growing nucleus and vice versa [56]. The atom undergoing transition from matrix with the high dislocation density to the recrystallised grain obtains the additional propelling force of a big value F_{rb} (b - atom volume) if the propelling force F_r acts on the recrystallisation front. Therefore, the recrystallisation front migration movement rate is:

$$v = bv_D c_v \left\{ \exp\left(-\frac{\Delta G_m}{kT}\right) - \exp\left[-\frac{\Delta G_m + F_r b^3}{kt}\right] \right\} \quad (3)$$

where:

v_D - Debye frequency equal to $10^{13} s^{-1}$,

c_v - concentration of vacancies at the grains boundary,

k - Boltzman constant,

T - temperature, K.

The propelling force of the primary recrystallisation, assuming that the dislocation density in cold worked metal is

$\rho_p \approx 10^{15}-10^{16} \text{ m}^{-2}$ and gets smaller down to $\rho_r \approx 10^{10} \text{ m}^{-2}$ after the recrystallization front passes and taking into account that energy per dislocation unit length is αGb^2 , is given by the relationship [56]:

$$F_r \approx \alpha Gb^2 (\rho_p - \rho_r) \quad (4)$$

where:

G - modulus of rigidity

b- dislocation Burgers vector

α - constant with the value from 0.5 to 1, depending on dislocation orientation

The single recrystallisation nuclei, being in fact proof of commencing the recrystallisation process in the deformation bands areas, were observed during ageing at temperature of 400°C in CuTi2,42 alloy microstructure as soon as after 1 hour. Rising the ageing temperature to 600°C results in the intensity increase and cutting the time of the recrystallisation process in the deformation bands areas, which is completed already after 1 minute of ageing [12].

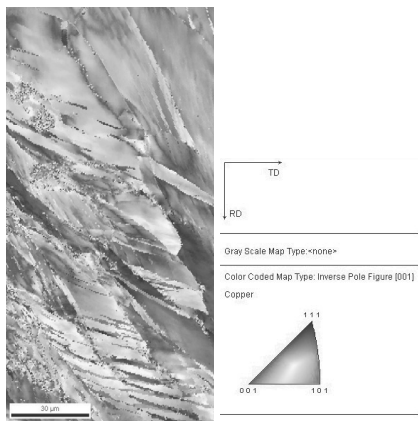


Fig. 9. EBSD analysis results, texture representation (reverse pole figure) of the alloy aged at temperature of 550°C for 1 min

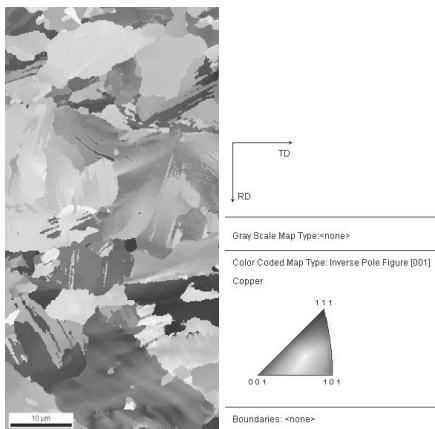


Fig. 10. EBSD analysis results, texture representation (reverse pole figure) of the alloy aged at temperature of 550°C for 60 min

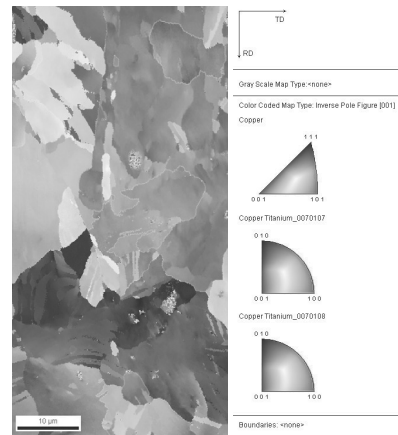


Fig. 11. EBSD analysis results, texture representation (reverse pole figure) of the alloy aged at temperature of 550°C for 420 minutes

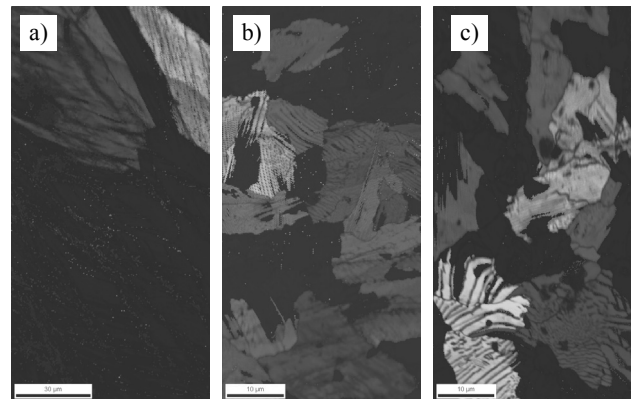


Fig. 12. Microstructure of CuTi4 alloy aged at temperature of 550°C for a) 1 min, b) 60 min, c) 420 min, grains size

At the successive investigation phase the qualitative X-ray phase analysis was carried out of the CuTi4 alloy hot worked with $Z=80\%$ draft, supersaturated next (920°C/1 h) in water, and cold worked next with $Z=50\%$ draft and aged at temp. 550°C for 1, 30, 60, 150, and 420 minutes. Analysis results are presented in Table 8. Apart from values of angles for the occurring peaks maximums the potential phases are also specified which are characteristic for the particular 2θ angle value.

Table 5. CuTi4 alloy (supersaturated - cold worked), aged at 550°C for 1 min (Fig. 7a)

	Grain size [μm]		Portion [%]
	min	min	
■	0.74	22.25	66.4
■	22.25	31.46	3.4
■	31.46	38.52	7.7
■	38.52	44.48	0
■	44.48	49.73	15.1

Table 6.

CuTi4 alloy (supersaturated - cold worked), aged at 550°C for 60 min (Fig. 7b)











	Grain size [μm]		Portion [%]
	min	min	
	0.29	8.61	45.3
	8.61	12.17	27.5
	12.17	14.91	5.1
	14.91	17.21	0
	17.21	19.24	21.5

Table 7.

CuTi4 alloy (supersaturated - cold worked), aged at 550°C for 420 min (Fig. 7c)

	Grain size [μm]		Portion [%]
	min	max.	
	0.222	8.54	46.0
	8.54	12.08	17.6
	12.08	14.80	23.5
	14.80	17.08	0.0
	17.08	19.10	11.6

Based on the qualitative X-ray phase analysis presence of phases: copper Cu (111), (200), (220), (311), and (222), Cu_3Ti (200), (211) was found in the CuTi4 alloy after hot working with 80% draft, supersaturation at temp. 930°C/1h and cooling in water, with the succeeding cold working with 50% draft (Fig. 13). No changes in structure were found after supersaturation for 1, 10, 15 or 30 minutes (Fig. 14).

As the phase detection threshold of the X-ray phase analysis is 3% of the mass fraction, the absence of Cu_4Ti phase means that this phase did not precipitate during that short ageing time or else that only its negligible amount precipitated. After ageing for 60 and 120 minutes the Cu_4Ti (020), (211) phase precipitated, which is connected with hardness growth of the investigated alloys, which was confirmed in [16]. However, ageing for 420 minutes causes dissolving of Cu_4Ti particles, which is attested by the X-ray photograph (Fig. 15). One can clearly see that intensity of peaks got reduced nearly to the background level. This results with hardness reduction when mechanical properties are concerned [16].

The Cu_4Ti particles with long range ordering (LRO) precipitating during ageing of CuTi alloys [57] are responsible for

Table 8.

Results of the X-ray phase analysis of CuTi4 alloy hot worked with 80% draft supersaturated at temp. 930°C/1h, and next cold worked with 50% draft and finally supersaturated at temp. 550°C for 1, 30, 60, 120, and 420 minutes

Ageing time of CuTi4 alloy at temperature of 550°C									Potential phases				
unaged [2 θ]	1 min [2 θ]	10 min [2 θ]	15 min [2 θ]	30 minut [2 θ]	60 minutes [2 θ]	120 minut [2 θ]	420 minut [2 θ]						
					48.88	48.76			Cu_2Ti , CuTi- γ , Cu_4Ti , Cu_3Ti , Cu_3Ti - β				
					53.38	53.27			Cu_4Ti , Cu_3Ti - β				
50.50	50.50	50.76	50.76	50.70	50.70	50.70	50.70		Cu				
					59.13	59.33	59.33	59.33	Cu, Cu_4Ti_3				
					88.40	88.42	88.76	88.81	88.77	88.77	88.77	88.77	Cu, Cu_3Ti
									94.52			CuTi - γ , Cu_3Ti , Cu_3Ti - β	
					109.64	109.49	110.21	110.26	110.31	110.26	110.20	110.28	Cu, Cu_3Ti , Cu_3Ti - β
					117.22	117.57	117.96	117.96		117.76	117.87	117.93	Cu

precipitation hardening in the heat treated copper alloys. This phase crystallizes in $D1_a$ system, yet the identity periods were described for the body-centred orthorhombic crystal system, however the base cell crystallizes in the body-centred tetragonal crystal system of Ni_4Mo , type, space group $I4/m$ [46]. No Cu_4Ti precipitations were revealed in the investigated alloys after ageing for 1, 10, 15, and 30 minutes (Fig. 14).

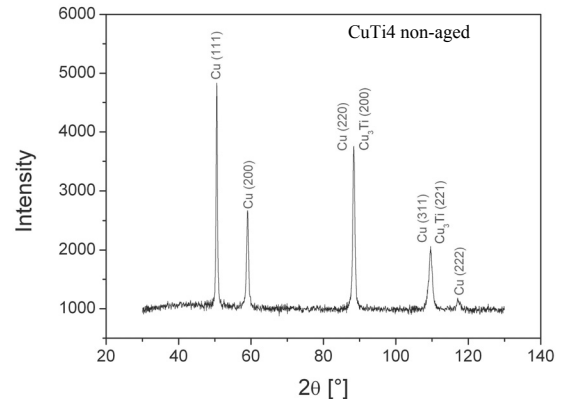


Fig. 13. Diffraction pattern of the qualitative X-ray phase analysis of CuTi4 alloy hot worked with 80% draft supersaturated at temp. 930°C/1h, cold worked next with 50% draft

The relationship of precipitation incubation time t_w o with temperature is described with the following formula [58]:

$$t_w = A(c) \exp \frac{Q_D + Q_Z(T, c)}{kT} \quad (5)$$

where:

A(c) - coefficient depending on concentration of impurities c; taking into account the propelling force of the reaction, transformation entropy, and geometry factor.

Q_D - diffusion activation energy of the dissolved element atoms;
 $Q_Z(T, c)$ - nucleation activation energy of the second phase changes from infinity (at equilibrium temperature) to very small values (with significant superfusions)

k - Boltzman constant,
 T - absolute temperature.

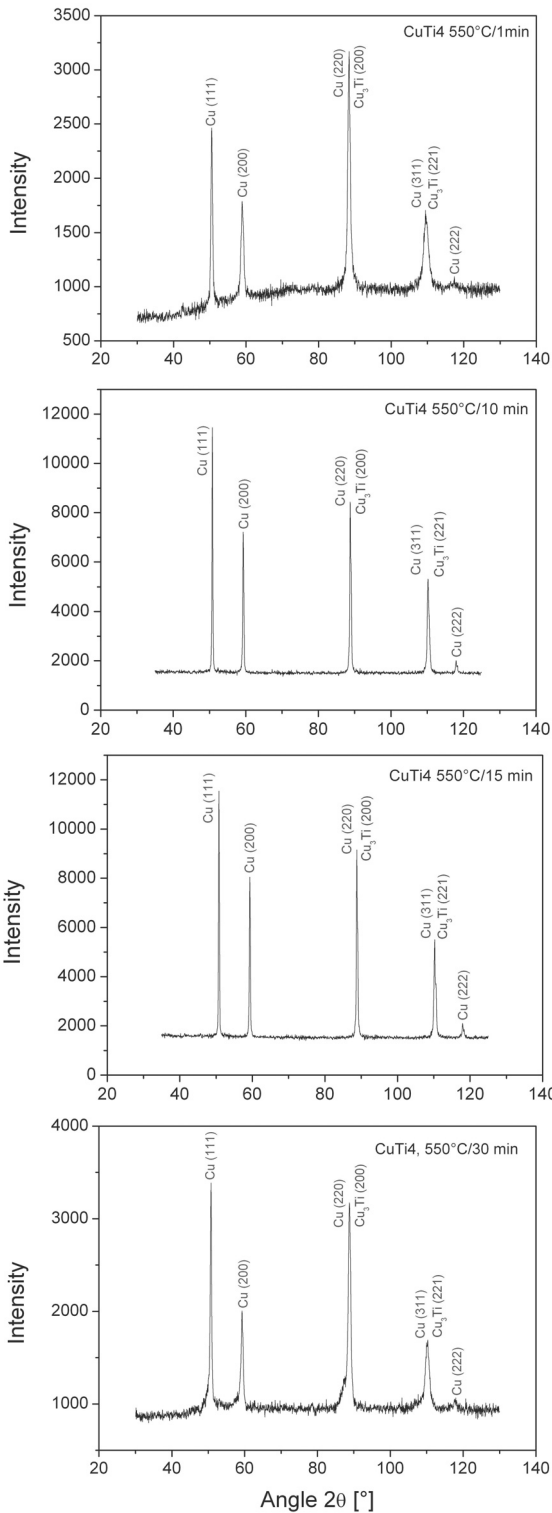


Fig. 14. Diffraction patterns of the qualitative X-ray phase analysis of CuTi4 alloy hot worked with 80% draft, supersaturated at temp. 930°C/1h, and next cold worked with 50% draft and finally supersaturated at temp. 550°C for 1, 10, 15 and 30 min

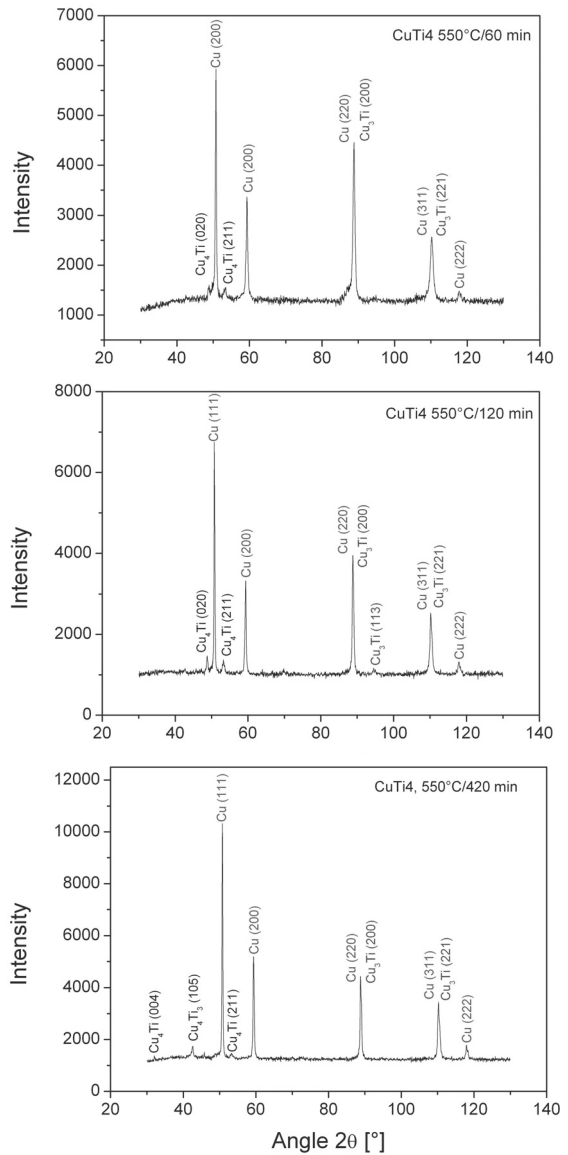


Fig. 15. Diffraction patterns of the qualitative X-ray phase analysis of CuTi4 alloy hot worked with 80% draft, supersaturated at temp. 930°C/1 h, and next cold worked with 50% draft and finally supersaturated at temp. 550°C for 60, 120 and 420 minutes

Next, incubation time of recrystallisation t_R depending on temperature is described by the relationship [59]:

$$t_R = B(\rho) \exp \frac{Q(\rho)}{kT} \quad (6)$$

where:

$B(\rho)$ - coefficient depending on density of dislocations and their spatial distribution, engaging strength of propellants recrystallization, the entropy term and geometric factor,

$Q(\rho)$ - activation energy of the recrystallisation nuclei forming, decreasing with the dislocation density growth.

Next, in Figure 16, the summary diffraction pattern is shown for ageing times of 1, 60, 120, and 420 minutes, in which one can clearly notice the growing intensity of peaks coming from Cu and Cu_3Ti . One can also see occurrences of peaks from Cu_4Ti after 60 minutes of ageing and growth of their intensity after 120 minutes of ageing, and next the partial decline or reduction of intensity of peaks after 420 minutes of ageing.

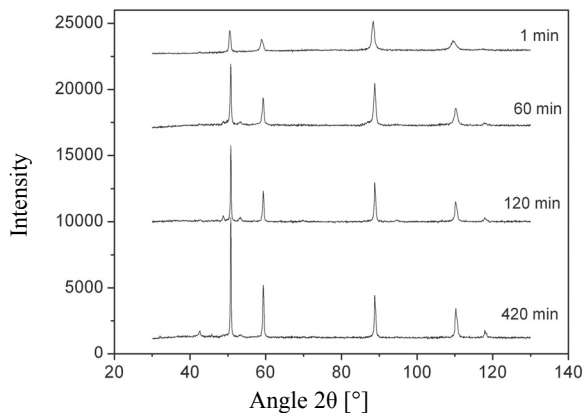


Fig. 16. Diffraction patterns of the qualitative X-ray phase analysis of CuTi4 alloy hot worked with 80% draft, supersaturated at temp. 930°C/1h, and next cold worked with 50% draft and finally supersaturated at temp. 550°C for 1, 60, 120 and 420 minutes

Kinetics of the modulation wave length change attests to the spinodal nature of the transformation occurring in CuTi alloys during ageing.

$$\lambda_m = k \cdot t^{0.16} \quad (7)$$

where:

k - constant,

t - ageing time.

In case of the cold worked CuTi alloys after supersaturation and next aged the modulation wave length grows significantly slower than in the undeformed alloys. Effect of deformation between the heat treatment operations is described by the following empirical equation:

$$\lambda_m = k \cdot t^{0.09} \quad (8)$$

Reduction of the kinetics growth of modulation width in the plastic deformed CuTi alloys is caused by the heterogeneous nucleation of phases on dislocations. They interact very strongly

and impede titanium concentration growth in modulations, and therefore change of amplitude and modulation wave length.

Kinetics of phase transformations in Cu-Ti alloys were characterised using the structural X-ray analysis methods, as well as with the transmission - and scanning electron microscopy. Investigation results confirmed unambiguously that the modulated microstructure forms during ageing of Cu-Ti alloys. Changes of the chemical composition do not have a sinusoidal character [12].

Because of the discontinuous transformation Cu_3Ti phase precipitates in the form of lamellae arranged alternately with the solid solution lamellae (Fig. 17). Because of the spinodal transformation the coherent precipitations were formed distributed periodically in the matrix. Chemical composition of the equilibrium phase and microstructure are not determined unambiguously. Two forms of the equilibrium phase are distinguished: the unordered phase β' and the ordered phase β . Phase β' crystallizes in the rhombic crystal system with lattice parameters:

$$a = 0.2572 - 0.2585 \text{ nm}$$

$$b = 0.4503 - 0.4527 \text{ nm}$$

$$c = 0.4313 - 0.4351 \text{ nm}$$

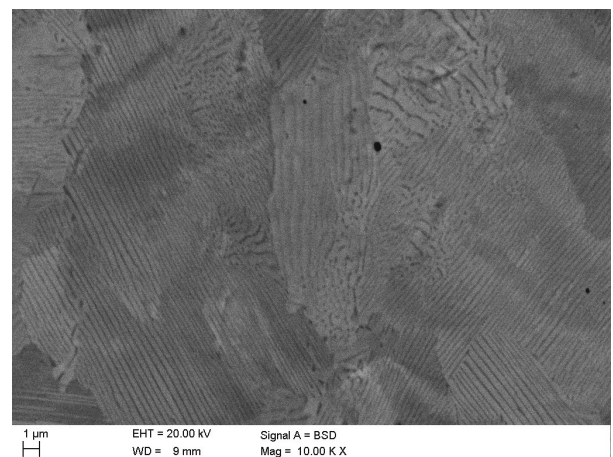


Fig. 17. Microstructure of CuTi4 alloy aged at temperature of 550°C for 420 minutes, visible lamellar precipitations; SEM

Based on values of lattice parameters of phase β' content of titanium was determined which is in the range of 21-25% at. and the Cu_3Ti stoichiometric formula was assigned to it. For 25% at. titanium concentration the lattice parameters correspond to the lattice parameters of the A3 hexagonal structure with the compact, densely packed lattice.

$$a = 0.262 \text{ nm}$$

$$b = 0.453 \text{ nm}$$

$$c = 0.427 \text{ nm}$$

Values of the lattice parameter a compared to phase β which crystallizes in the rhombic crystal system is twice as big than the identity period a of phase β' (Fig. 18).

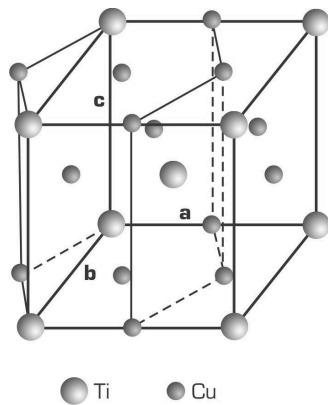


Fig. 18. Mutual orientation of elementary cells of phase β' (hexagonal) and phase β (rhombic) [54]

It was found, based in microstructure analysis with EBSD, that along with the ageing time of CuTi4 alloy, the portion of the small-angle boundaries from the range of 2-15° gets smaller, being for 1, 60, and 420 minutes of ageing equal to 61.1, 26.5, and 9.1% respectively, whereas the portion of the high-angle boundaries from the range of 15-180° grows, being for 1, 60, and 420 minutes of ageing equal to 38.9, 72.5, and 90.9% respectively. Increase the participation of a wide-angle boundaries conclusively demonstrates an advanced process of twinning as a result of extending the aging time.

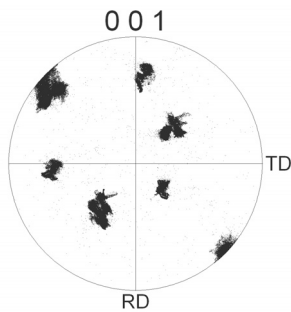


Fig. 19. Pole figure of microstructure of the CuTi4 alloy aged at temperature of 550°C for 1 min

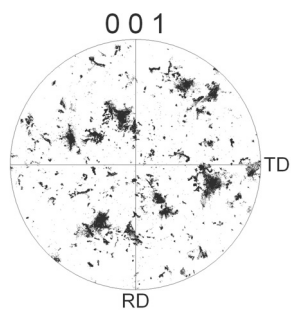


Fig. 20. Pole figure of microstructure of the CuTi4 alloy aged at temperature of 550°C for 60 minutes

Using the planar pole figures texture was presented of CuTi4 alloy hot worked with 80% draft supersaturated at temp. 930°C/1h, and next cold worked with 50% draft and finally supersaturated at temp. 550°C for 1, 60, and 420 minutes (Figs. 19-21). In the investigated alloy, like in other metals and alloys crystallizing in the cubic lattice Al and with EBU smaller than $(30-40) \cdot 10^{-3} \text{ J/m}^2$ texture $\{110\}\langle 112 \rangle$ was formed called the alloy texture (or the brass one). Copper has big EBU (about $60 \cdot 10^{-3} \text{ J/m}^2$) and therefore during rolling at ambient temperature in Cu the pure metal texture is formed - copper texture. Usually is described in the simplest form by the ideal orientation $(123)[42\bar{1}]$ or as a combination of orientations $(146)[2\bar{1}\bar{1}]$ and $(123)[4\bar{1}\bar{2}]$.

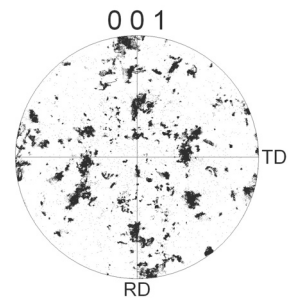


Fig. 21. Pole figure of microstructure of the CuTi4 alloy aged at temperature of 550°C for 420 min

Thanks to introducing to copper elements reducing EBU of the solid solution continuous transition is possible from copper texture to alloy texture. Also deformation temperature change may cause transformation of one orientation into another one. For an example, rolling at low temperature may cause transition of copper texture into brass one. On the other hand the reverse transformation is obtained by rolling at the temperature range of 150-200°C.

4. Conclusions

The presented structure investigations results for the CuTi4 industrial alloy after heat treatment (supersaturation 20°C/1 h./water + 50% draft + ageing 550°C/ 1 min and 550°C/420 min) display the significant differences in the microstructure of the investigated alloy. In particular, microstructure of alloys aged at temp. 550°C for 1 minute is reach in deformation twins bands (Fig. 2) and also start of the spinodal transformation was revealed, whose effect are the continuous- and discontinuous precipitation areas (Figs. 4, 5). However, in the microstructure of the alloy aged at temp. 550°C for 420 minutes presence of titanium particles $\text{Ti}\alpha$ was revealed as deformation twins (Fig. 6), and also the Cu matrix deformation twins (Fig. 7).

It was found, based in microstructure analysis with EBSD, that along with the ageing time of CuTi4 alloy, the portion of the small-angle boundaries from the range of 2-15° gets smaller, being for 1, 60, and 420 minutes of ageing equal to 61.1, 19.3, and 15.8% respectively, whereas the portion of the high-angle boundaries from the range of 15-180° grows, being for 1, 60, and

420 minutes of ageing equal to 38.9, 80.7, and 84.2% respectively. Increase the participation of a wide-angle boundaries testifies to the ongoing process of twinning, whose intensity increases with increasing aging time.

Next, measurement results of grain size with the EBSD method showed unambiguously that along with the ageing time growth in the investigated range of CuTi4 alloy supersaturated 920°C/1 h/water + cold worked with 50% draft + ageing 550°C/ 1, 60, and 420 minutes occurs the primary recrystallisation phenomenon realised by the mechanism of nucleation of new grains.

It was revealed using the qualitative X-ray phase analysis that the metastable Cu₄Ti₁ phase, which is responsible in CuTi alloys for the precipitation hardening effect, precipitated in the investigated alloy after ageing for 60 and 120 minutes. Extension of the ageing time caused dissolving of the Cu₄Ti phase particles.

Investigations carried out revealed that the structural phenomena occurring during heat treatment of the cold worked metals and alloys do not allow to separate recovery from recrystallisation [60]. However, as the continuous recrystallisation process proceeds without movement of the high-angle grain boundaries, one may infer, based on the obtained results that in the ageing process at the temperature of 550°C/420 minutes, nucleation of new grains and twinning during aging are the dominating mechanism.

References

- [1] W. Ozgovicz, E. Kalinowska-Ozgowicz, B. Grzegorzczk, Thermomechanical treatment of low-alloy copper alloys of the kind CuCo2Be and CuCo1NiBe, *Journal of Achievements in Materials and Manufacturing Engineering* 46/2 (2011) 161-168.
- [2] W. Głuchowski, J.P. Stobrawa, Z.M. Rdzawski, K. Marszowski, Microstructural characterization of high strength high conductivity Cu-Nb microcomposite wires, *Journal of Achievements in Materials and Manufacturing Engineering* 46/1 (2011) 40-49.
- [3] S.J. Skrzypek, W. Ratuszek, A. Bunsch, M. Witkowska, J. Kowalska, M. Goły, K. Chruściel, Crystallographic texture and anisotropy of electrolytic deposited copper coating analysis, *Journal of Achievements in Materials and Manufacturing Engineering* 43/1 (2010) 264-268.
- [4] W. Głuchowski, J.P. Stobrawa, Z.M. Rdzawski, Microstructure refinement of selected copper alloys strips processed by SPD method, *Archives of Materials Science and Engineering* 47/2 (2011) 103-109.
- [5] A.D. Dobrzańska-Danikiewicz, K. Lukaszowicz, Technology validation of coatings deposition onto the brass substrate, *Archives of Materials Science and Engineering* 46/1 (2010) 5-38.
- [6] J. Romanowska, L. Bencze, A. Popovic, Thermodynamic properties of liquid Cu-Sb-Sn alloys by equilibrium saturation and Knudsen effusion mass spectrometric methods, *Archives of Materials Science and Engineering* 39/2 (2009) 69-74.
- [7] J. Dutkiewicz, F. Masdeu, P. Malczewski, A. Kukula, Microstructure and properties of $\alpha+\beta$ brass after ECAP processing, *Archives of Materials Science and Engineering* 39/2 (2009) 80-83.
- [8] J.P. Stobrawa, Z.M. Rdzawski, Precipitation process of the Ni₃Al phase in copper-based alloys, *Journal of Achievements in Materials and Manufacturing Engineering* 15/1-2 (2006) 21-26.
- [9] Z. Gronostajski, K. Jaśkiewicz, Influence of monotonic and cyclic deformation sequence on behavior of CuSi3.5 silicon bronze, *Journal of Achievements in Materials and Manufacturing Engineering* 15/1-2 (2006) 39-46.
- [10] J.P. Stobrawa, Z.M. Rdzawski, Deformation behaviour of dispersion hardened nanocrystalline copper, *Journal of Achievements in Materials and Manufacturing Engineering* 17/1-2 (2006) 153-156.
- [11] L.A. Dobrzański, *Metal engineering materials*, WNT, Warsaw, 2004 (in Polish).
- [12] Z. Rdzawski, *Alloyed copper*, University of Technology Publishing House, Gliwice, 2009.
- [13] S. Bzowski, S. Gorczyca, Kinetics of homogeneous transformations in solid solutions with cubic lattice, *Metalurgia* 29 (1981) 33 (in Polish).
- [14] S. Nagarjuna, M. Srinivas, Grain refinement during high temperature tensile testing of prior cold worked and peak aged Cu-Ti alloys, Evidence of superplasticity, *Materials Science and Engineering A* 498 (2008) 468-474.
- [15] S. Nagarjuna, U. Chinta Babu, P. Ghosal, Effect of cryorolling on age hardening of Cu-1.5Ti alloy, *Materials Science and Engineering A* 491 (2008) 331-337.
- [16] Z. Rdzawski, J. Stobrawa, W. Głuchowski, J. Konieczny, Thermomechanical processing of CuTi4 alloy, *Journal of Achievements in Materials and Manufacturing Engineering* 42 (2010) 9-25.
- [17] S. Bzowski, S. Gorczyca, Phase changes in copper-titanium alloys, *Metallurgy* 29 (1981) 79-113.
- [18] M.J. Saarivirta, H.S. Cannon, Copper-titanium alloys, *Metal Progress* 76 (1959) 81-84.
- [19] J.A. Cornie, A. Datta, W.A. Soffa, An electron microscopy study of precipitation in Cu-Ti sideband alloys, *Metallurgical Transactions* 4 (1973) 727-733.
- [20] K. Sato, Direct Observations on precipitation in copper-titanium alloys, *Transactions of the Japan Institute of Metals* 7 (1966) 267-272.
- [21] A. Datta, W.A. Soffa, The structure and properties of age hardened Cu-Ti alloys, *Acta Metallurgica* 24/11 (1976) 987-1001.
- [22] R. Knights, P. Wilkes, The precipitation of titanium in copper and copper-nickel base alloys, *Acta Metallurgica* 21 (1973) 1503-1514.
- [23] D.E. Laughlin, J.W. Cahn, The crystal structure of the metastable precipitate in copper-based copper-titanium alloys, *Scripta Materialia* 8 (1974) 75-78.
- [24] D.E. Laughlin, J.W. Cahn, Communication, Ordering in copper titanium alloys, *Metallurgical Transactions* 5 (1974) 972-974.
- [25] T. Hakkarainen, Doctor of Technology Thesis, Helsinki, University of Technology, 1971.
- [26] L. Blacha, G. Siwiec, A. Kościelna, A. Dudzik-Truś, Effect of titanium content on microstructure and properties of alloys of Cu-Ti, *Materials Engineering* 1 (2010) 42-45 (in Polish).

- [27] T. Radetic, V. Radmilovic, W.A. Soffa, Electron microscopy observations of deformation twinning in a precipitation hardened copper-titanium alloy, *Scripta Materialia* 35/12 (1996) 1403-1409.
- [28] S. Semboshi, T. Al.-Kassab, R. Gemma, R. Kirchheim, Microstructural evolution of Cu-1 at% Ti alloy aged in a hydrogen atmosphere and its relation with the electrical conductivity, *Ultramicroscopy* 109 (2009) 593-598.
- [29] L. Blacha, G. Siwec, A. Kościelna, A. Dudzik-Truś, Effect of titanium content on microstructure and properties of alloys of Cu-Ti system, *Materials Engineering* 6 (2009) 520-524 (in Polish).
- [30] S. Nagarjuna, M. Srinivas, K. Balasubramanian, D.S. Sarma, The alloy content and grain size dependence of flow stress in Cu-Ti alloys, *Acta Materialia* 44/6 (1996) 2285-2293.
- [31] L. Blacha, W. Szkliniarz, G. Siwec, A. Kościelna, Effect of fabrication parameters in quality of ingots from Cu-Ti alloys, *Ores And Non-Ferrous Metals* 53/12 (2008) 784-789 (in Polish).
- [32] D. Watanabe, Ch. Watanabe, R. Monzen, Effect of coherency on coarsening of second-phase precipitates in Cu-base alloys, *Journal of Materials Science* 43 (2008) 3946-3953.
- [33] A.A. Hamed, L. Blaz, Microstructure of hot-deformed Cu-3.45 wt.% Ti alloy, *Materials Science and Engineering A* 254 (1998) 83-89.
- [34] H.T. Michels, I.B. Cadoff, E. Levine, Precipitation hardening in Cu-3.6wt.% Ti, *Metallurgical Transactions* 31 (1972) 667-74.
- [35] J. Dutkiewicz, Spinodal decomposition, ordering, and discontinuous precipitation in deformed and aged copper-titanium alloys, *Met Technology* 5 (1978) 333-340.
- [36] S. Nagarjuna, K. Balasubramanian, D.S. Sarma, Effects of cold work on precipitation hardening of Cu-4.5 mass% Ti alloy, *Materials Transactions* 36/8 (1995) 1058-66.
- [37] M.J. Saarivirta, H.S. Canon, Copper-titanium alloys have high strength, *Metal Progress* 76 (1959) 81-84.
- [38] N. Karlsson, An X-ray study of the phases in the copper-titanium system. *Journal Institute of Metals* 79 (1951) 391-405.
- [39] T.B. Massalski, *Binary alloys phase diagrams*, 1990.
- [40] J. Dutkiewicz, Spinodal- and discontinuous transformation mechanism and ordering processes in aged alloys with Al lattice, *Scientific Papers of AGH, Metallurgy and Foundry* No 80, Cracow, 1977 (in Polish).
- [41] J. Dutkiewicz, L. Lityńska, Employment of electron diffraction for investigation of spinodal transformation in Cu-Ti and Al-Zn alloys, *Proceedings of the 5th Conference on Electron Microscopy of Solids*, Warsaw-Jadwisin, 1978, 149-154 (in Polish).
- [42] J. Dutkiewicz, Spinodal decomposition, ordering and discontinuous precipitation in deformed and aged copper-titanium alloys, *Metals Technology* (1978) 333-340.
- [43] J. Dutkiewicz, L. Lityńska, Ordering within precipitates in copper-nickel-titanium alloys, *Journal of Materials Science* 15 (1980) 2307-2310.
- [44] G. Gottstein, *Rekristallisation metallischer Werkstoffe*, Deutsche Gesellschaft für Metallkunde, Germany, 1984.
- [45] J. Stobrawa, Role of the electric strain energy in forming structure and morphology of coherent precipitations in selected copper alloys, *Scientific Letters of Silesian University of Technology*, Gliwice, 2004 (in Polish).
- [46] P. Villars, L.D. Calvert, *Pearson's Handbook of crystallographic data for intermetallic phases IV*, ASM International, Ohio, 1991.
- [47] H.X. Li, X.J. Hao, G. Zhao, S.M. Hao, Characteristics of the continuous coarsening and discontinuous coarsening of spinodally decomposed Cu-Ni-Fe alloy, *Journal of Materials Science* 36 (2001) 779-784.
- [48] J.-C. Zhao, M.R. Notis, Spinodal decomposition, ordering transformation, and discontinuous precipitation in a Cu-15Ni-8Sn alloy, *Acta Materialia* 46/12 (1998) 4203-4218.
- [49] M.A. Mangan, G.J. Shiflet, Tree dimensional investigation of CuTi discontinuous precipitation, *Scripta Materialia* 37/4 (1997) 517-522.
- [50] I.K. Razumov, Formation of intermediate ordered states on spinodal decomposition of alloys, *Journal of Engineering Physics and Thermophysics* 81/4 (2008) 826-833.
- [51] V. Sofonea, K.R. Meeke, Morphological characterization of spinodal decomposition kinetic, *The European Physical Journal B* 8 (1999) 99-112.
- [52] V. Daniel, H. Lipson, An X-ray study of the dissociation of an alloy of copper, iron and nickel, *London A* 181/987 (1943) 368-378.
- [53] V. Lebreton, D. Pachoutinski, Y. Bienvenu, An investigation of microstructure and mechanical properties in Cu-Ti-Sn alloys rich in copper, *Materials Science and Engineering A* 508 (2009) 83-92.
- [54] P. Prasad Rao, B.K. Agrawal, A.M. Rao, Comparative study of spinodal decomposition in symmetric and asymmetric Cu-Ni-Cr alloys, *Journal of Materials Science* 26 (1991) 1485-1496.
- [55] H.-W. Kim, S.-B. Kang, N. Tsuji, Y. Minamino, Elongation in increase in ultra-fine Al-Fe-Si alloy sheets, *Acta Materialia* 54 (2006) 1785.
- [56] J. Adamczyk, *Theoretical physical metallurgy, Plastic strain, strengthening, and cracking*, University of Technology Publishing House, Gliwice, 2005 (in Polish).
- [57] Wei Yinghui, Wang Xiaotian, A new ordered phase forming during ageing in Cu-Ti alloys, *Chinese Science Bulletin*, 42/19 (1997) 1671-1672.
- [58] E. Hornbogen, U. Köster, *Recrystallization of Metallic Materials*, F. Haesner (Ed.), Verlag, Berlin, 1978, 159.
- [59] E. Hornbogen, H. Kreye, *Textures in research and practice*, J. Grewen, G. Wassermann (Ed.), Springer-Verlag, Berlin 1969.
- [60] M. Blicharski, S. Gorczyca, *Recrystallisation with participation of the second phase*, "Śląsk" Publishing House, Katowice, 1980 (in Polish).